JOURNAL OF MATERIALS SCIENCE 21 (1986) 260–268

Preparation of nickel-based amorphous alloys with finely dispersed lead and lead–bismuth particles and their superconducting properties

A. INOUE, M. OGUCHI*, K. MATSUZAKI‡, Y. HARAKAWA*, T. MASUMOTO
The Research Institute for Iron, Steel and Other Metals and ‡Graduate School, Department of Metallurgy, Tohoku University, Sendai 980, Japan

The application of the melt-quenching technique to Ni–Si–B–Pb, Ni–P–B–Pb, Ni–Si–B–Pb–Bi and Ni–P–B–Pb–Bi alloys containing immiscible elements such as lead and bismuth has been tried and it has been found to result in the formation of a new type of material consisting of fine fcc Pb or hcp ε(Pb–Bi) + bct X(Pb–Bi) particles dispersed uniformly in the nickel-based amorphous matrix. The particle size and interparticle distance were 1 to 3 and 1 to 4 μm, respectively, for the lead phase, and less than 0.2 to 0.5 μm and 0.2 to 1.0 μm for the Pb–Bi phase. The uniform dispersion of such fine particles into the amorphous matrix was achieved in the composition range below about 6 at% Pb and 7 at% (Pb + Bi). Additionally, these amorphous alloys have been found to exhibit a superconductivity by the proximity effect of fcc Pb or ε(Pb–Bi) superconducting particles. The transition temperature T_c was in the range 6.8 to 7.5 K for the Ni–Si(or P)–B–Pb alloys and 8.6 to 8.8 K for the Ni–Si (or P)–B–Pb–Bi alloys. The upper critical field H_{c2} and the critical current density J_c for $(Ni_{0.8}P_{0.1}B_{0.1})_{95}Pb_3Bi_2$ at 4.2 K were, respectively, about 1.6 T and of the order of 7×10^7 A m^{-2} at zero applied field. Melt quenching of amorphous phase-forming alloys containing an immiscible element has thus been demonstrated, enabling us to produce amorphous composite materials exhibiting unique and useful characteristics which cannot be obtained in homogeneous amorphous alloys.

1. Introduction

Up to this date, the preparation of an amorphous alloy by the melt-quenching technique has been very actively tried for quite a large number of alloy systems. However, almost all the compositions of their alloys have been focused [1] on the region near to the eutectic point in metal–metalloid systems and on the regions of eutectic point and stoichiometric compound in metal–metal systems. The selection of such alloy compositions has generally been believed due to the expectation of a great supercooling ability and an enhanced glass transition temperature, through strong metal–metalloid and metal–metal interactions. Surprisingly, there is no information available on the effect of melt-quenching on the microstructure and properties of alloys containing a solute element which is immiscible in the liquid or solid state with the constituent elements of the amorphous phase. This is probably because of a fear that the addition of the immiscible elements might result in a significant reduction of supercooling capacity in the alloy during melt-quenching.

The equilibrium phase diagram of the Ni–Pb system [2] indicates a great difficulty in obtaining a nickel alloy with a uniformly mixed structure of lead phase when the alloy is solidified at a normal cooling rate. However, there is a high possibility that the application of melt-quenching to the Ni–Si(or P)–B–Pb and Ni–Si(or P)–B–Pb–Bi alloys results in the formation of ductile nickel-based amorphous alloys with finely dispersed lead or lead–bismuth particles, so that their melt-quenched duplex alloys exhibit superconductivity by the proximity effect of superconducting lead or lead–bismuth particles, even though no superconductivity is expected for the Ni–Si–B and Ni–P–B amorphous alloys.

The aim of this paper is to examine the microstructure and superconducting properties of melt-quenched Ni–Si(or P)–B–Pb and Ni–Si(or P)–B–Pb–Bi alloys and to investigate the usefulness of the addition of small amounts of immiscible elements into the nickel-based amorphous alloys.

2. Experimental procedures

Alloys with the composition $(Ni_{0.75}Si_{0.08}B_{0.17})_{100-x}Pb_x$, $(Ni_{0.8}P_{0.1}B_{0.1})_{100-x}Pb_x$, $(Ni_{0.75}Si_{0.08}B_{0.17})_{100-x}(Pb_{0.6}Bi_{0.4})_x$ and $(Ni_{0.8}P_{0.1}B_{0.1})_{100-x}(Pb_{0.6}Bi_{0.4})_x$ were used in the present work. The alloy ingots were prepared by arc melting the mixture of the pre-alloyed Ni–Si–B or Ni–P–B ingots and pure lead and/or bismuth metals in a purified argon atmosphere. Typically, the amount of each ingot melted in one arc melting was about 2 g,

Permanent address: Research and Development, Teikoku Piston Ring Ltd, Okaya 394, Japan.

0022–2461/86 $03.00 + .12

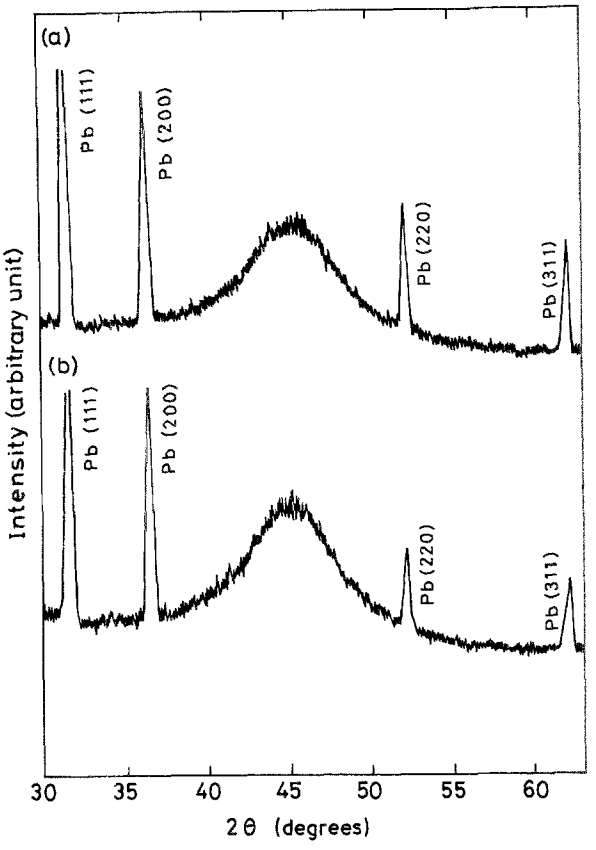

Figure 1 X-ray diffraction patterns showing the duplex structure consisting of amorphous and fcc lead phase in melt-quenched alloys: (a) $(Ni_{0.75}Si_{0.08}B_{0.17})_{95}Pb_5$ (a = 0.4957 nm), (b) $(Ni_{0.8}P_{0.1}B_{0.1})_{95}Pb_5$ (a = 0.4952 nm).

and the whole ingot was used in one melt-quenching operation to produce ribbon samples of about 2 mm width and 0.03 mm thickness in air by a single-roller spinning apparatus with a copper wheel ($\simeq$ 20 cm in diameter). The compositions of the alloys are nominal ones since the losses during melting were negligible. The as-quenched structure was examined by X-ray diffractometry, differential scanning calorimetry (DSC) and optical microscopy. Measurements of superconducting properties T_c, $J_c(H)$, $H_c(T)$ and $H_{c2}(T)$ were made by the d.c. method using four electrical probes. The temperature was measured with an accuracy of ± 0.01 K using a calibrated germanium thermometer. A magnetic field of up to 9 T was applied perpendicularly to the specimen surface and feed current.

3. Results

3.1. Melt-quenched structure

Fig. 1 shows the X-ray diffraction patterns of melt-quenched $(Ni_{0.75}Si_{0.08}B_{0.17})_{95}Pb_5$ and $(Ni_{0.8}P_{0.1}B_{0.1})_{95}Pb_5$ alloys. One can see some sharp diffraction peaks corresponding to lead as well as a broad peak of amorphous phase, indicating the formation of a coexistent structure of amorphous and lead phases. The lattice parameter of lead is 0.4957 nm for the Ni–Si–B–Pb alloy and 0.4952 nm for the Ni–P–B–Pb alloy, being nearly the same as that (0.49502 nm [3]) of pure lead. This indicates clearly that no dissolution of the other constituent elements (nickel, silicon, boron and phosphorous) into the lead phase takes place, as is expected from the equilibrium phase diagrams of Ni–Pb [2], Si–Pb [4] and B–Pb [5]. Optical micrographs presented in Fig. 2 show the distribution of the lead phase on the freely solidified surface of $(Ni_{0.75}Si_{0.08}B_{0.17})_{100-x}Pb_x$ and $(Ni_{0.8}P_{0.1}B_{0.1})_{100-x}Pb_x$ (x = 2.5 and 5.0) ribbon samples. It can be seen that the lead particles are uniformly dispersed in the amorphous

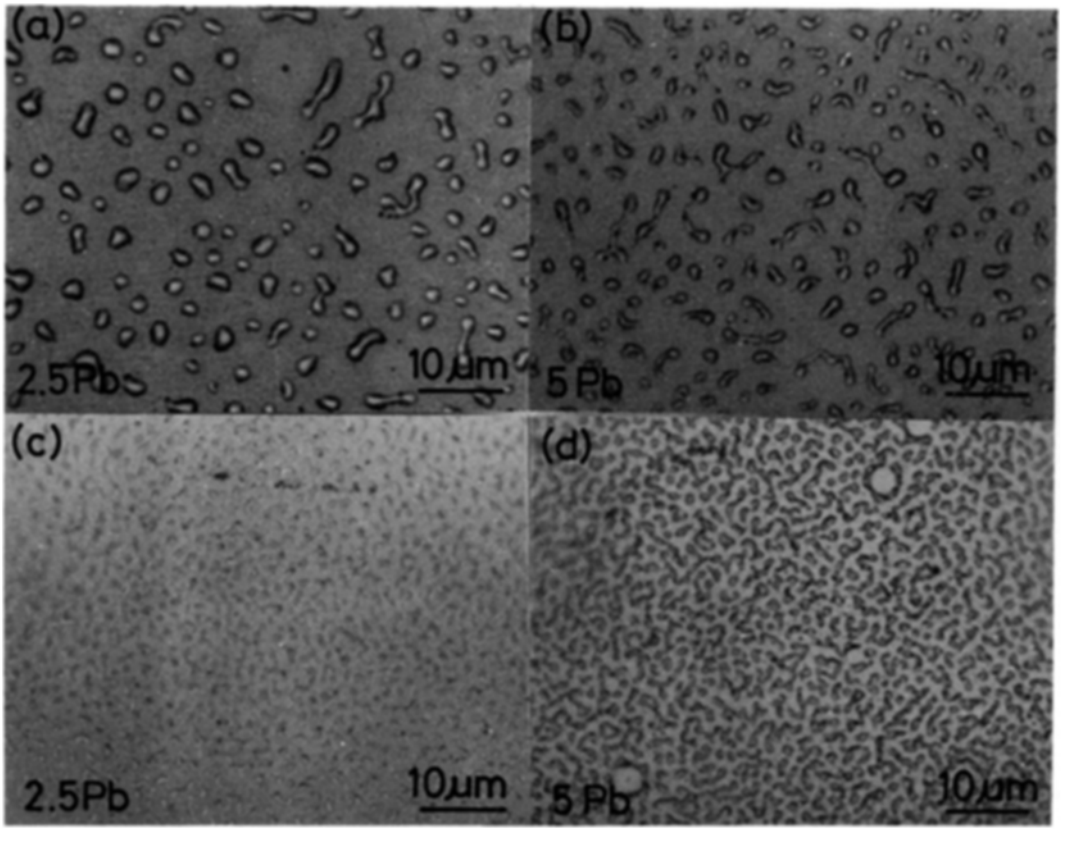

Figure 2 Optical micrographs showing the duplex structure consisting of amorphous and lead phase in melt-quenched alloys: (a) $(Ni_{0.75}Si_{0.08}B_{0.17})_{97.5}Pb_{2.5}$, (b) $(Ni_{0.75}Si_{0.08}B_{0.17})_{95}Pb_5$, (c) $(Ni_{0.8}P_{0.1}B_{0.1})_{97.5}Pb_{2.5}$ and (d) $(Ni_{0.8}P_{0.1}B_{0.1})_{95}Pb_5$.

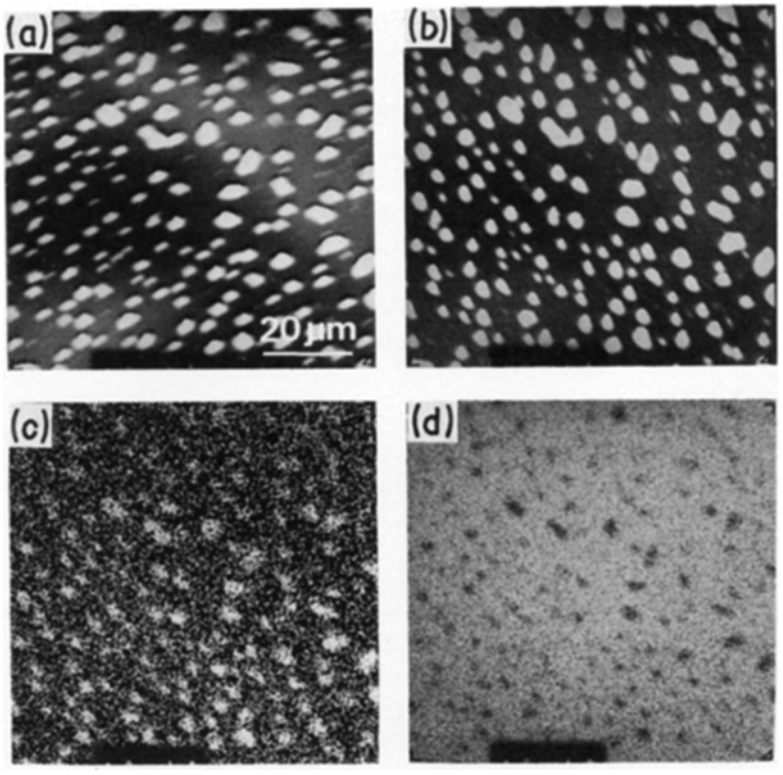

Figure 3 Scanning electron micrographs showing (a) topological and (b) compositional states on the free surface of melt-quenched $(Ni_{0.75}Si_{0.08}B_{0.17})_{95}Pb_5$ ribbon, and X-ray images showing the distribution of (c) lead and (d) nickel.

matrix. The average lead particle size is 1.5 to 3.0 μm for the former alloys and 1.0 to 1.5 μm for the latter alloys. Although there is no appreciable change in the particle size with lead content, the interparticle distance tends to decrease slightly from 3.0 to 4.0 μm at 2.5% Pb to 2.5 to 3.5 μm at 5.0% Pb for the Ni–Si–B–Pb alloys, and from 1.0 to 1.5 μm at 2.5% Pb to 0.8 to 1.5 μm at 5.0% Pb for the Ni–P–B–Pb alloys. In order to confirm the distribution of alloy components in the amorphous matrix and lead precipitates, X-ray diffraction images of nickel and lead were examined for the present duplex alloys. As an example, Fig. 3 shows the scanning electron topological image (Fig. 3a) and compositional image (Fig. 3b), and X-ray images showing the distribution of lead (Fig. 3c) and nickel (Fig. 3d). The results in Fig. 3 allow us to confirm that the second-phase particle is lead and the matrix is the nickel-based amorphous phase.

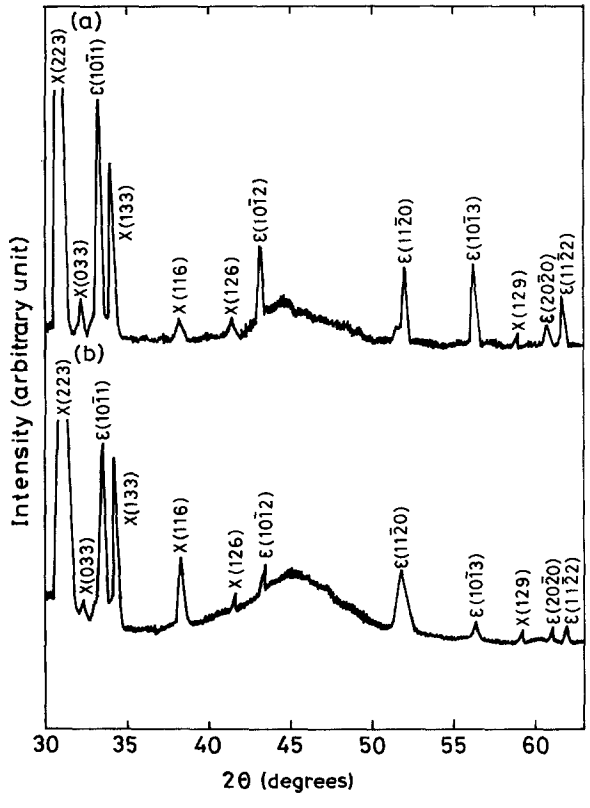

Figure 4 X-ray diffraction patterns showing the mixed structure consisting of amorphous, h c p ε(Pb–Bi) and b c t X(Pb–Bi) phases in melt-quenched alloys: (a) $(Ni_{0.75}Si_{0.08}B_{0.17})_{95}Pb_3Bi_2$, (b) $(Ni_{0.8}P_{0.1}B_{0.1})_{95}Pb_3Bi_2$. For h c p ε, a = 0.350 nm and c = 0.579 nm; for b c t X, a = 0.993 nm and c = 1.449 nm.

A similar coexistent structure of amorphous phase and immiscible metal was also obtained for Ni–Si–B–Pb–Bi and Ni–P–B–Pb–Bi alloys, as shown in Figs. 4 and 5. The precipitates in the alloys containing both lead and bismuth consist of the two phases of an h c p ε phase with a = 0.350 nm and c = 0.579 nm, and a b c t X phase with a = 0.993 nm and c = 1.449 nm. The ε phase is a supersaturated solid solution of the equilibrium h c p phase which exists in the range 24 to 33 at % Bi at room temperature [6, 7], and the X-phase is a non-equilibrium phase which appears only in the rapidly solidified case [8]. Furthermore, one can see in Fig. 5 that the simultaneous addition of lead and bismuth results in a further reduction in the particle size of the immiscible phases, e.g., 0.2 to 0.5 μm for $(Ni_{0.75}Si_{0.08}B_{0.17})_{95}Pb_3Bi_2$, and the ε and X precipitates in $(Ni_{0.8}P_{0.1}B_{0.1})_{95}Pb_3Bi_2$ alloy are too fine to distinguish their particles by optical microscopy. Here it appears important from an engineering point of view to point out that all the duplex alloy ribbons containing less than about 6 at % Pb or 7 at % (Pb + Bi) possess a good bending ductility as shown by 180° bending.

3.2. Superconducting properties

Typical examples of the normalized electrical resistance (R/R_n) curves in the vicinity of T_c in the case of no

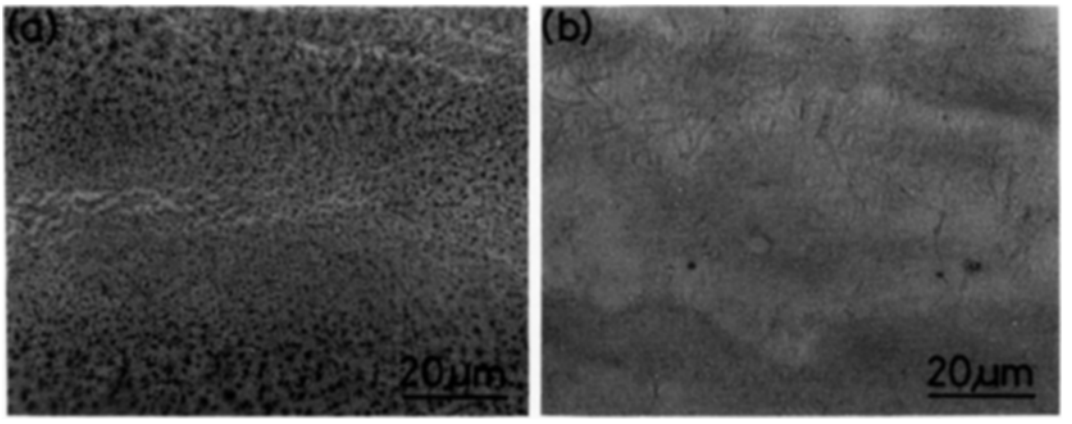

Figure 5 Optical micrographs showing the mixed structure consisting of amorphous, ε(Pb–Bi) and X(Pb–Bi) phases in melt-quenched alloys: (a) $(Ni_{0.75}Si_{0.08}B_{0.17})_{95}Pb_3Bi_2$, (b) $(Ni_{0.8}P_{0.1}B_{0.1})_{95}Pb_3Bi_2$.

applied magnetic field are shown in Fig. 6 for $(Ni_{0.75}Si_{0.08}B_{0.17})_{100-x}Pb_x$, in Fig. 7 for $(Ni_{0.8}P_{0.1}B_{0.1})_{100-x}Pb_x$ and in Fig. 8 for $(Ni_{0.75}Si_{0.08}B_{0.17})_{95}Pb_3Bi_2$ and $Ni_{0.8}P_{0.1}B_{0.1})_{95}Pb_3Bi_2$. Here R_n is the resistance in the normal state. The transition occurs rather sharply with a temperature width (ΔT_c) of less than 0.80 K for the lead-containing alloys and less than 0.35 K for the alloys containing lead and bismuth. The transition temperature T_c, which was taken as the temperature at $R/R_n = 0.5$, is 6.8 K for Ni–Si–B–2.5Pb, 7.1 K for Ni–Si–B–5Pb, 7.2 K for Ni–P–B–2.5Pb, 7.5 K for Ni–P–B–5Pb, 8.6 K for Ni–Si–B–3Pb–2Bi and 8.8 K for Ni–P–B–3Pb–2Bi. From these data, the following description may be derived: (a) T_c for the alloys containing lead and bismuth is higher by 1.1 to 2.0 K than that of the alloys containing only lead, (b) the increase in lead content from 2.5 to 5.0% results in a rise of T_c by about 0.3 K, and (c) T_c is higher for the Ni–P–B–Pb(or Pb–Bi) alloys than for the Ni–Si–B–Pb(or Pb–Bi) alloys. Additionally, whilst the variation with temperature of the normal electrical resistivity for the Ni–Si–B–Pb and Ni–P–B–Pb alloys is positive and the slope is rather large, no variation is seen for the Ni–Si(or P)–B–Pb–Bi alloys in the temperature range below 17 K. Thus, the temperature dependence of normal electrical resistivity is significantly different between the Ni–Si(or P)–B–Pb alloys and the Ni–Si (or P)–B–Pb–Bi alloys.

The critical magnetic field, H_c, was measured at various temperatures ranging from 1.5 K to T_c. Fig. 9 shows the transition curves from the superconducting state to the normal state at different temperatures at a current density of $6.0 \times 10^4 A\,m^{-2}$ for $(Ni_{0.8}P_{0.1}B_{0.1})_{95}Pb_5$ and $2.5 \times 10^6 A\,m^{-2}$ for $(Ni_{0.8}P_{0.1}B_{0.1})_{95}Pb_3Bi_2$. Resistive states for the former alloy are limited to an extremely narrow range of fields (0.01 to 0.03 T), in strong contrast with a relatively wide range (0.09 to 0.27 T) for the latter alloy. Such a markedly different transition behaviour is thought to reflect the difference in the type (I or II) of their superconductors. Here we define H_c and H_{c2} to be the applied magnetic fields at which the resistance of the samples begins to deviate from its normal value. The temperature dependence of H_c is shown in Fig. 10 for $(Ni_{0.8}P_{0.1}B_{0.1})_{95}Pb_5$, and that of H_{c2} is shown in Fig. 11 for $(Ni_{0.75}Si_{0.08}B_{0.17})_{95}Pb_3Bi_2$ and $(Ni_{0.8}P_{0.1}B_{0.1})_{95}Pb_3Bi_2$, where the solid lines represent a linear extrapolation at T_c. H_c increases linearly with falling temperature over almost the whole temperature range and the gradient at T_c, $-(dH_{c2}/dT)_{T_c}$, is 5.99×10^{-3} T K^{-1} for the Ni–P–B–Pb alloy, 0.17 T K^{-1} for the Ni–Si–B–Pb–Bi alloy and 0.16 T K^{-1} for the Ni–P–B–Pb–Bi alloy. It is thus noticed that the gradient for the alloys containing lead and bismuth is higher by a factor of 32 to 34 than that of the lead-containing alloy through the difference in the type of their superconductors, i.e., Type I for lead and

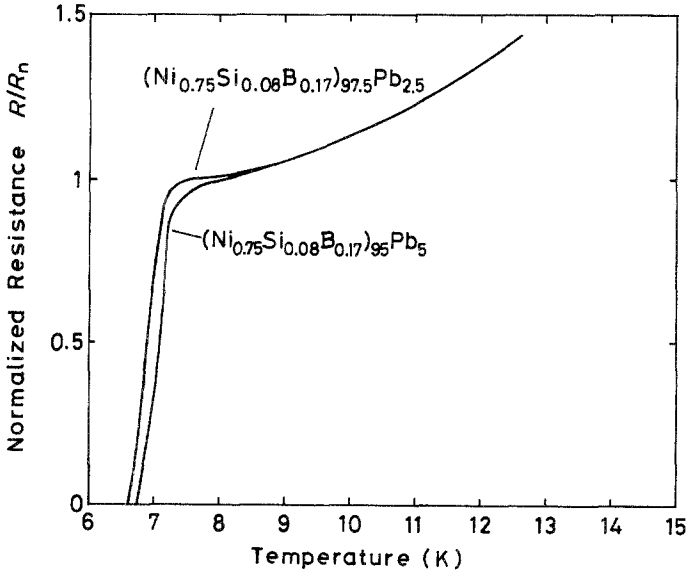

Figure 6 Normalized resistance ratio R/R_n as a function of temperature for melt-quenched alloys $(Ni_{0.75}Si_{0.08}B_{0.17})_{100-x}Pb_x$ (x = 2.5 and 5.0) possessing coexisting amorphous and lead phases.

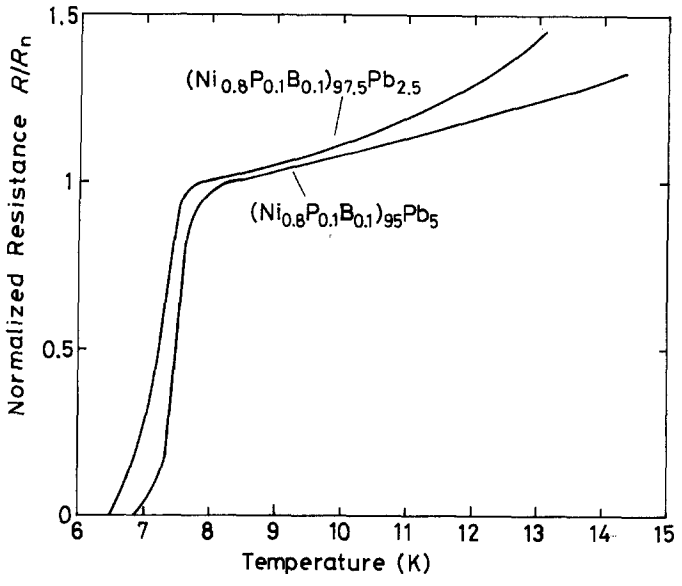

Figure 7 Normalized resistance ratio R/R_n as a function of temperature for melt-quenched alloys $(Ni_{0.8}P_{0.1}B_{0.1})_{100-x}$-$Pb_x$ (x = 2.5 and 5.0) possessing coexisting amorphous and lead phases.

Type II for lead–bismuth [9]. As is expected from the marked difference in the gradient, the critical field at 4.2 K is 0.046 T for the Ni–P–B–Pb alloy which is much lower than those (1.4 to 1.6 T) found for the Ni–P(or Si)–B–Pb–Bi alloys.

The critical current density, J_c, was measured at 4.27 K and 2.86 K under an external applied magnetic field for $(Ni_{0.8}P_{0.1}B_{0.1})_{95}Pb_3Bi_2$, the alloy exhibiting the highest T_c among all the alloys examined in the present work. J_c as a function of external applied field is plotted in Fig. 12. The value of J_c in the absence of applied field is about $7 \times 10^7 A m^{-2}$ at 4.27 K and $1.5 \times 10^8 A m^{-2}$ at 2.86 K, and the value decreases rapidly with increasing applied field. For example, at $H = 1.2$ T, J_c is of the order of $8.3 \times 10^5 A m^{-2}$ at 4.27 K and $8.0 \times 10^6 A m^{-2}$ at 2.86 K. The relatively high values of J_c at $H = 0$ are probably due to the lead–bismuth dispersed particles in the amorphous matrix acting as effective pinning centres, owing to the particle size being comparable to the coherence length ($\simeq 20$ nm) [10] and the existence of a high density of quenched-in defects in lead–bismuth alloy particles. The fluxoid pinning force F_p evaluated from the data in Fig. 12 is plotted as a function of reduced magnetic field H/H_{c2} in Fig. 13, where F_p is calculated as $H \times J_c$. The maximum F_p and the value of H/H_c where F_p shows a maximum value are, respectively, $1.5 \times 10^7 N m^{-3}$ and 0.26 at 4.27 K and $2.5 \times 10^7 N m^{-3}$ and 0.31 at 2.86 K. These values are much larger than those ($\simeq 10^4 N m^{-3}$ and 0.2) [11] for homogeneously amorphous superconductors without effective fluxoid pinning centres.

4. Discussion

In this section, we shall firstly consider the reason why the duplex structure containing a small amount of lead or lead–bismuth particles in the nickel-based amorphous matrix results in an appearance of superconductivity, despite the fact that the homogeneously amorphous nickel-based alloys do not exhibit superconductivity even at a temperature as low as 50 mK [12]. Judging from the micrographs shown in Figs. 2 and 5, it is concluded that the present appearance of superconductivity for the nickel-based amorphous alloys containing lead or lead–bismuth particles is due to the proximity effect which results from lead or lead–bismuth superconducting particles embedded in the amorphous matrix. The nominal composition and

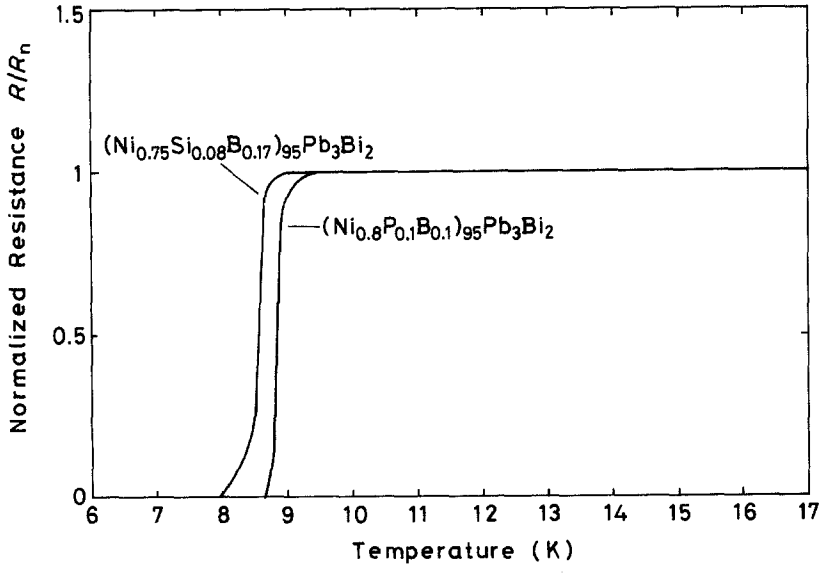

Figure 8 Normalized resistance ratio R/R_n as a function of temperature for melt-quenched alloys $(Ni_{0.75}Si_{0.08}B_{0.17})_{95}Pb_3Bi_2$ and $(Ni_{0.8}P_{0.1}B_{0.1})_{95}Pb_3Bi_2$ possessing coexisting amorphous, hcp ε(Pb–Bi) and bct X(Pb–Bi) phases.

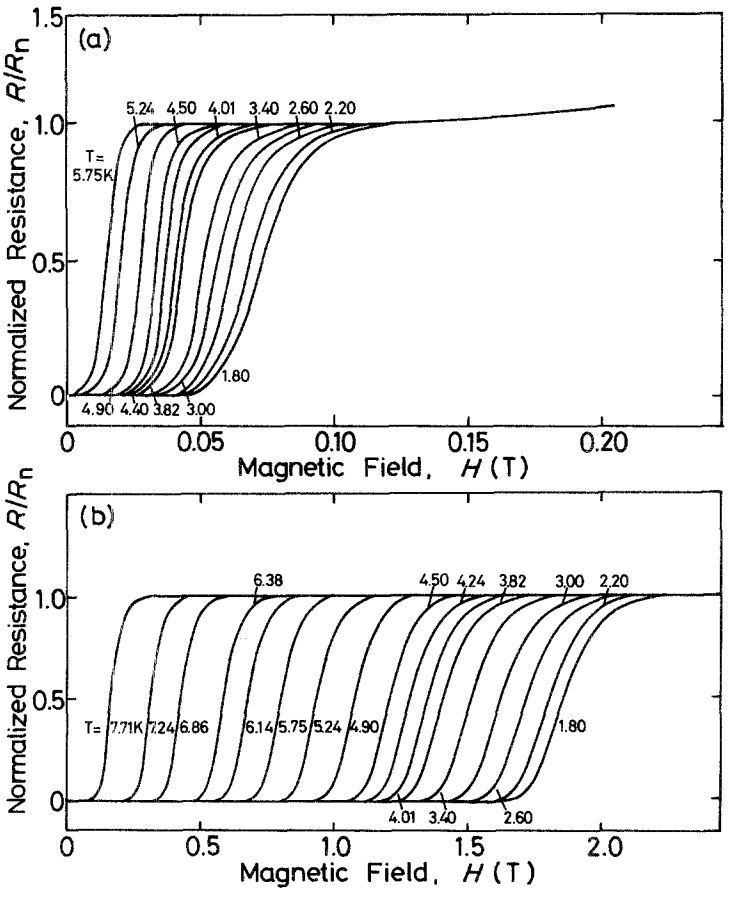

Figure 9 Normalized resistance ratio R/R_n as a function of magnetic field at various temperatures for melt-quenched alloys possessing coexisting amorphous and lead or ε(Pb–Bi) + X(Pb–Bi) phases: (a) $(Ni_{0.8}P_{0.1}B_{0.1})_{95}Pb_5$, (b) $(Ni_{0.8}P_{0.1}B_{0.1})_{95}Pb_3Bi_2$.

T_c of the duplex alloys and the particle radius (r) and interparticle distance (λ) of lead and lead–bismuth phases are summarized in Table I, where λ implies the distance between the centres of their particles. The residual electrical resistivity of $Ni_{75}Si_8B_{17}$ and $Ni_{80}P_{10}B_{10}$ amorphous alloys at 4.2 K was measured to be about 1.80 $\mu\Omega$ m and 1.85 $\mu\Omega$ m, respectively. From these values of electrical resistivity, the mean free path of electrons (l) is estimated to be about 1 nm from the nearly-free electron model [13]. Further, the coherence length (ξ_0) of amorphous superconductors has

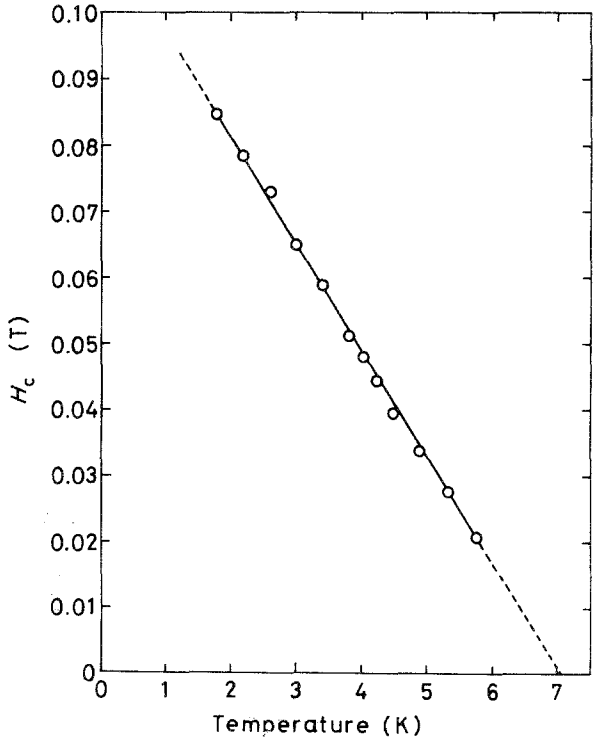

Figure 10 The critical magnetic field H_c at various temperatures for melt-quenched $(Ni_{0.8}P_{0.1}B_{0.1})_{95}Pb_5$ alloy possessing coexisting amorphous and lead phases. The solid line represents a linear extrapolation near T_c.

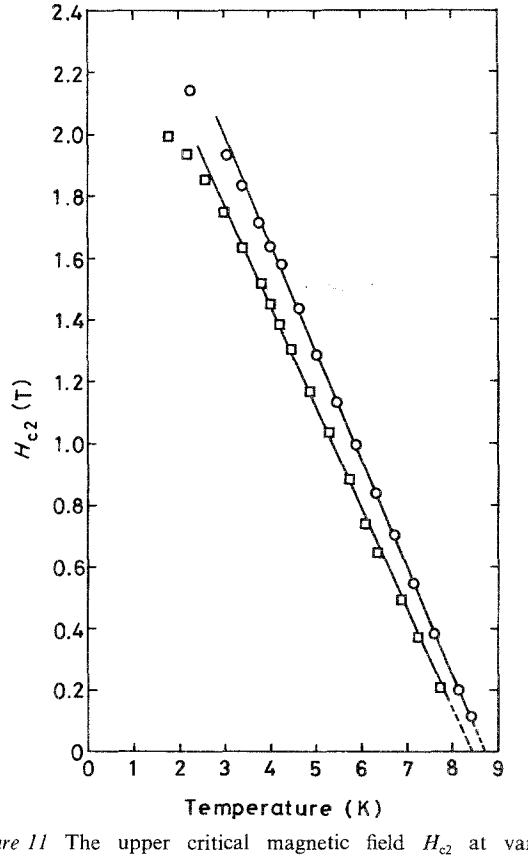

Figure 11 The upper critical magnetic field H_{c2} at various temperatures for melt-quenched alloys possessing coexisting amorphous, hcp ε(Pb–Bi) and bct X(Pb–Bi) phases: (○) $(Ni_{0.75}Si_{0.08}B_{0.17})_{95}Pb_3Bi_2$, (□) $(Ni_{0.8}P_{0.1}B_{0.1})_{95}Pb_3Bi_2$. The solid lines represent a linear extrapolation near T_c.

TABLE I As-quenched structure, the particle size $2r$ and interparticle distance λ of lead and lead–bismuth phases embedded in amorphous matrix, the superconducting transition temperature T_c, the transition width ΔT_c, the critical field gradient at T_c, $-(dH_{c2}/dT)_{T_c}$, the critical field at 4.2 K, the residual electrical resistivity ϱ_n and the ratio r/ξ_0 of particle radius to the coherence length of lead or ε(Pb–Bi), for melt-quenched $(Ni_{0.75}Si_{0.08}B_{0.17})_{100-x}Pb_x$, $(Ni_{0.8}P_{0.1}B_{0.1})_{100-x}Pb_x$, $(Ni_{0.75}Si_{0.08}B_{0.17})_{95}Pb_3Bi_2$ and $(Ni_{0.8}P_{0.1}B_{0.1})_{95}Pb_3Bi_2$ alloys possessing coexisting amorphous and lead or ε(Pb–Bi) + X(Pb–Bi) phases

Alloy	$2r$ (μm)	λ (μm)	T_c (K)	ΔT_c (K)	$-(dH_{c2}/dT)_{T_c}$ (TK^{-1})	H_c or H_{c2} at 4.2 K (T)	ϱ_n ($\mu\Omega$ m)	r/ξ_0
$(Ni_{0.75}Si_{0.08}B_{0.17})_{97.5}Pb_{2.5}$	1.5 to 2.5	3.0 to 4.0	6.8	0.47	–	–	0.19	9.0 to 15
$(Ni_{0.75}Si_{0.08}B_{0.17})_{95}Pb_5$	1.5 to 3.0	2.5 to 3.5	7.1	0.73	–	–	0.17	9.0 to 18
$(Ni_{0.8}P_{0.1}B_{0.1})_{97.5}Pb_{2.5}$	1.0 to 1.5	1.0 to 1.5	7.2	0.80	–	–	0.21	6.0 to 9.0
$(Ni_{0.8}P_{0.1}B_{0.1})_{95}Pb_5$	1.0 to 1.5	0.8 to 1.5	7.5	0.55	5.99×10^{-3}	0.046	0.64	6.0 to 9.0
$(Ni_{0.75}Si_{0.08}B_{0.17})_{95}Pb_3Bi_2$	0.2 to 0.5	0.2 to 0.7	8.6	0.35	0.17	1.6	1.70	8.7 to 22
$(Ni_{0.8}P_{0.1}B_{0.1})_{95}Pb_3Bi_2$	–	–	8.8	0.18	0.16	1.4	2.00	–

generally been reported [14, 15] to be of the order 50 to 100 nm from the data for low-temperature specific heat and magnetic susceptibilities. Since the mechanism for the appearance of superconductivity by the proximity effect has been considered [16] to be dominated by the characteristics of the matrix phase, the present duplex alloys consisting of amorphous and lead or lead–bismuth phase can therefore be classified to be typical of dirty superconductors because $l \ll \xi_0$ for the amorphous matrix.

For the proximity effect in the case of the dirty limit, the leak distance (K_n^{-1}) is expressed [16] by

$$K_n^{-1} = (h v_n l_n / 6\pi k_B T)^{1/2}$$

Here v_n and l_n are the Fermi velocity and the mean free path, respectively, of electrons in normal conducting alloy. The above equation indicates that K_n^{-1} is influenced only by the electrons in normal conducting alloy (matrix phase). K_n^{-1} for the amorphous matrix phase is very small because of the small l_n value, and hence the superconducting lead and lead–bismuth particles must disperse closely to each other to exhibit a high T_c by the proximity effect. Additionally, it has been shown [17] that the critical radius of superconducting lead or lead–bismuth particle (r_c) for the proximity effect in the case of $L = l/\xi = 1$ must be above $2.965\xi_0^*$, where ξ is the BCS coherence length of the matrix phase and ξ_0^* is the coherence length of the lead or lead–bismuth particle. The ξ_0^* value has been reported to be 83 nm for pure lead [18] and 23 nm for $Pb_{80}Bi_{20}$ [19]. As a result, r_c is estimated to be about 250 nm for lead and about 70 nm for $Pb_{60}Bi_{40}$, if one assumes that the ξ_0 value of $Pb_{60}Bi_{40}$ particles is nearly the same as that of $Pb_{80}Bi_{20}$ alloy. This estimate indicates that the radii of lead and $Pb_{60}Bi_{40}$ particles must be larger than about 250 and 70 nm, respectively, for achieving high T_c values by the proximity effect, in addition to a very short leak distance.

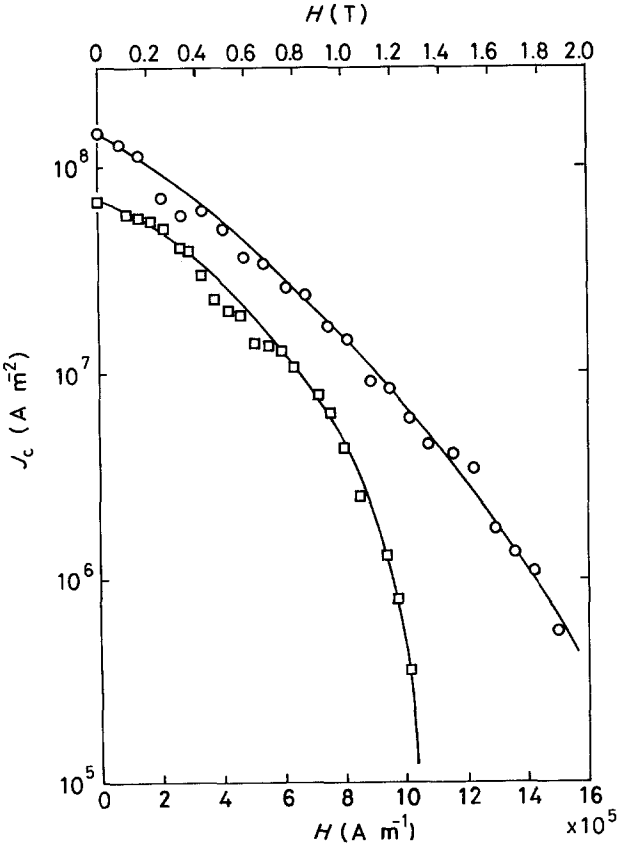

Figure 12 Critical current density J_c as a function of magnetic field for melt-quenched $(Ni_{0.8}P_{0.1}B_{0.1})_{95}Pb_3Bi_2$ alloy possessing coexisting amorphous, hcp ε(Pb–Bi) and bct X(Pb–Bi) phases: (○) 2.86 K, (□) 4.27 K.

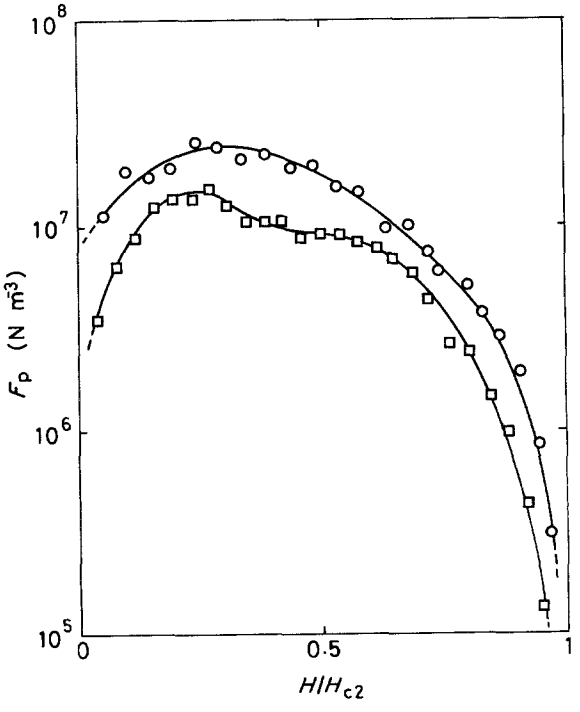

Figure 13 Fluxoid pinning force F_p as a function of reduced magnetic field H/H_{c2} for melt-quenched $(Ni_{0.8}P_{0.1}B_{0.1})_{95}Pb_3Bi_2$ alloy possessing coexisting amorphous, hcp ε(Pb–Bi) and bct X(Pb–Bi) phases: (○) 2.86 K, (□) 4.27 K.

As summarized in Table I, the particle radius of lead and $Pb_{60}Bi_{40}$ phases is about 3 to 6 r_c for the Ni–Si–B–Pb alloys, 2 to 3 r_c for the Ni–P–B–Pb alloys, 1.5 to 3.5 r_c for the Ni–Si–B–Pb–Bi alloy and smaller than 1.5r_c for the Ni–P–B–Pb–Bi alloy. Theoretical analyses [17] on the variation of normalized transition temperature (T_c/T_{cl}) of duplex alloys as a function of r/ξ_0^* suggest that the T_c/T_{cl} value is in the range 0 to 0.50 for the Ni–Si–B–Pb alloys and zero for the other Ni–P–B–Pb, Ni–Si–B–Pb–Bi and Ni–P–B–Pb–Bi alloys. Here T_{cl} is the superconducting critical temperature of lead metal or $Pb_{60}Bi_{40}$ alloy itself. Nevertheless, the actually measured T_c values (6.8 to 8.8 K) of these duplex alloys are much higher than the theoretically expected values (0 to 3.6 K), implying that the real critical radii of superconducting lead and $Pb_{60}Bi_{40}$ particles in the duplex alloys are much smaller than the estimated values.

The reason for such a remarkable difference is considered to be due to the fact that the present duplex alloy superconductors are extremely dirty because of an amorphous structure of the matrix phase. For such an extremely dirty superconductor, the degree of dirtiness defined by $L = l/\xi$ is estimated to be as small as about 0.01, and hence the real critical radius of the duplex alloys is calculated to be about $0.225\xi_0^*$ from Silvert's analysis [20, 21] as shown in Fig. 14. It is worth noting that the value is much smaller than the radius ($2.965\xi_0^*$) calculated by the assumption [17] of $L = 1$. Under the assumption that the L value is 0.01 for the present Ni–Si–B and Ni–P–B amorphous alloys, the T_c/T_{cl} value is theoretically estimated [20, 21] to be 1.0 for $(Ni_{0.75}Si_{0.08}B_{0.17})_{95}Pb_5$, 1.0 for $(Ni_{0.8}P_{0.1}B_{0.1})_{95}Pb_5$, 0.98 to 1.0 for $(Ni_{0.75}Si_{0.08}B_{0.17})_{95}Pb_3Bi_2$, and smaller than 0.98 for $(Ni_{0.8}P_{0.1}B_{0.1})_{95}Pb_3Bi_2$ from the actually measured $R = r/\xi_0^*$ values, as plotted in Fig. 14. It is noted that the estimated values are nearly the same as the actually measured T_c values for the melt-quenched alloys. Accordingly, the reason why the duplex alloys exhibit almost the same T_c values as those of pure lead metal or $Pb_{60}Bi_{40}$ alloy in spite of the small sizes of the dispersed particles is reasonably thought to originate from the extreme dirtiness of the amorphous matrix phase.

As shown in Figs. 10 and 11, the temperature gradient of H_c and H_{c2} near T_c is 5.99×10^{-3} T K^{-1} for $(Ni_{0.8}P_{0.1}B_{0.1})_{95}Pb_5$, 0.17 T K^{-1} for $(Ni_{0.75}Si_{0.08}B_{0.17})_{95}Pb_3Bi_2$, and 0.16 T K^{-1} for $(Ni_{0.8}P_{0.1}B_{0.1})_{95}Pb_3Bi_2$, and the critical magnetic field at 4.2 K is 0.046 T for the Ni–P–B–Pb alloy, 1.6 T for the Ni–Si–B–Pb–Bi alloy and 1.4 T for the Ni–P–B–Pb–Bi alloy. Thus, the critical fields of the latter two alloys are larger by a factor of about 33 than that of the former. The remarkable difference is thought to originate from an inherent difference in the mechanism of superconductivity; the superconductivity of the Ni–Si(or P)–B–Pb duplex alloys is due to the proximity effect of lead particles which are Type I superconductors, whereas that of the Ni–Si(or P)–B–Pb–Bi duplex alloys is due to that of the Type II Pb–Bi superconductor. Additionally, the actually observed H_c ($\simeq 0.046$ T at 4.2 K) for $(Ni_{0.8}P_{0.1}B_{0.1})_{95}Pb_5$ is nearly equal to the previously reported H_c ($\simeq 0.047$ T) of pure lead [19], but the measured H_{c2} values ($\simeq 1.4$ to 1.6 T at 4.2 K) for the Ni–Si–B–Pb–Bi and Ni–P–B–Pb–Bi alloys are higher by a factor of about three than the reported value ($\simeq 0.53$ T at 4.2 K) [19] of $Pb_{60}Bi_{40}$ alloy itself, despite the result that the appearance of the present superconductivity is due to the proximity effect of lead–bismuth alloy particles.

The value of H_{c2} is closely related to the dirtiness of the superconductor as well as T_c and the coefficient of low-temperature electronic specific heat (γ), and the larger the T_c, γ and residual resistivity ϱ_n the larger is H_{c2} [22]. Consequently, the achievement of such high H_{c2} values for the present Ni–Si(or P)–B–Pb–Bi duplex alloys is probably due to the high ϱ_n values of 1.70 to 1.98 $\mu\Omega$ m for the Ni–Si(or P)–B–Pb–Bi alloys which are generated by the introduction of a high density of internal faults and large internal strain into lead–bismuth alloy particles by melt-quenching, in addition to the high T_c values comparable to that (8.6 K [19]) of pure $Pb_{60}Bi_{40}$ alloy. Furthermore, it has been seen that the H_c value of the Ni–P–B–Pb alloy is nearly the same as that of conventionally solidified lead. This enables us to infer that the lead particles imbedded in the Ni–P–B amorphous alloy do not contain a high density of quenched-in defects. This inference is consistent with the result that ϱ_n for the Ni–P(or Si)–B–Pb alloys is as small as 0.17 to

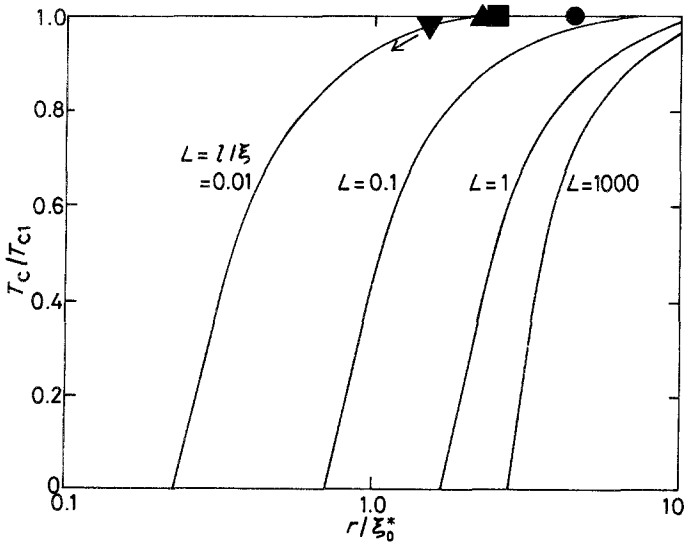

Figure 14 Theoretically estimated T_c/T_{cl} values as a function of r/ξ_0^* for melt-quenched alloys possessing coexisting amorphous and lead or ε(Pb–Bi) + X(Pb–Bi) phases: (●) $(Ni_{0.75}Si_{0.08}B_{0.17})_{95}Pb_5$, (■) $(Ni_{0.8}P_{0.1}B_{0.1})_{95}Pb_5$, (▲) $(Ni_{0.75}Si_{0.08}B_{0.17})_{95}Pb_3Bi_2$, (▼) $(Ni_{0.8}P_{0.1}B_{0.1})_{95}Pb_3Bi_2$. Symbols represent the average r/ξ_0^* values of each alloy.

0.21 $\mu\Omega$ m, being almost comparable to that of conventionally cast lead. The remarkable differences in critical magnetic field and ϱ_n between the Ni–Si(or P)–B–Pb and Ni–Si(or P)–B–Pb–Bi alloys remind us that a structural modification by melt-quenching is effective only for alloys consisting of two or more alloying elements.

5. Summary

Duplex amorphous alloys exhibiting superconductivity and high ductile nature were produced in $(Ni_{0.75}Si_{0.08}B_{0.17})_{100-x}Pb_x$, $(Ni_{0.8}P_{0.1}B_{0.1})_{100-x}Pb_x$ (x = 2.5 and 5.0), $(Ni_{0.75}Si_{0.08}B_{0.17})_{95}Pb_3Bi_2$ and $(Ni_{0.8}P_{0.1}B_{0.1})_{95}Pb_3Bi_2$ alloys. The duplex alloys consisted of amorphous and lead or lead–bismuth (hcp ε + bct X) phases. The particle size and interparticle distances are 1 to 3 and 1 to 4 μm, respectively, for the Ni–Si(or P)–B–Pb alloys and less than 0.2 to 0.5 and 0.2 to 1.0 μm, respectively, for the Ni–Si(or P)–B–Pb–Bi alloys. The formation of amorphous alloys with uniformly dispersed lead or lead–bismuth particles was limited to less than about 6 at % Pb for the Ni–Si(or P)–B–Pb system and about 7 at % (Pb + Bi) for the Ni–Si(or P)–B–Pb–Bi system.

These duplex alloys were found to exhibit superconductivity by the proximity effect of finely dispersed lead or lead–bismuth particles at temperatures higher than 4.2 K. The transition temperature T_c tends to increase slightly with increasing volume fraction of lead and lead–bismuth phases, and reaches a maximum value of 7.1 K for $(Ni_{0.75}Si_{0.08}B_{0.17})_{95}Pb_5$, 7.5 K for $(Ni_{0.8}P_{0.1}B_{0.1})_{95}Pb_5$, 8.6 K for $(Ni_{0.75}Si_{0.08}B_{0.17})_{95}Pb_3Bi_2$ and 8.8 K for $(Ni_{0.8}P_{0.1}B_{0.1})_{95}Pb_3Bi_2$. The temperature gradient of critical magnetic field (H_c and H_{c2}) near T_c and the critical field at 4.2 K are 5.99×10^{-3} T K^{-1} and 0.046 T for $(Ni_{0.8}P_{0.1}B_{0.1})_{95}Pb_5$, and 0.16 T K^{-1} and 1.4 T for $(Ni_{0.8}P_{0.1}B_{0.1})_{95}Pb_3Bi_2$. The critical current density J_c is of the relatively high order of 7×10^7 A m^{-2} at zero applied field and 4.2 K for $(Ni_{0.8}P_{0.1}B_{0.1})_{95}Pb_3Bi_2$. It is thus very important from scientific and engineering points of view that the application of the melt-quenching technique to the nickel–metalloid alloys containing lead or (Pb + Bi) elements, which are immiscible in an equilibrium state against their consituent elements, results in the formation of a duplex structure consisting of fine lead or (Pb + Bi) particles dispersed uniformly in the nickel-based amorphous matrix, and their duplex alloys exhibit rather good superconducting properties combined with high hardness and good ductility. Further development of the ideas presented here seems to be capable of producing amorphous composite materials having unique characteristics which cannot be obtained in homogeneous amorphous alloys.

References

1. H. A. DAVIES, "Amorphous Metallic Alloys", edited by F. E. Lubrosky (Butterworths, London, 1983) p. 8.
2. M. HANSEN, "Constitution of Binary Alloys" (McGraw-Hill, New York, 1958) p. 1028.
3. W. B. PEARSON, "Handbook of Lattice Spacings and Structures of Metals and Alloys" (Pergamon Press, London, 1958) p. 803.
4. E. R. JETTE and E. B. GEBERT, *J. Chem. Phys.* **1** (1933) 735.
5. M. HANSEN, "Constitution of Binary Alloys" (McGraw-Hill, New York, 1958), p. 245.
6. D. SOLOMON and W. MORRIS-JONES, *Phil. Mag.* **11** (1931) 1090.
7. H. HOFE and H. HANEMANN, *Z. Metallkunde* **32** (1940) 112.
8. C. SURYANARAYANA and T. R. ANANTHARAMAN, *Solid State Commun.* **12** (1973) 87.
9. I. LIVINGSTON, *Phys. Rev.* **129** (1963) 1943.
10. H. RAFFY, J. C. RENARD and E. GUYON, *Solid State Commun.* **11** (1972) 1679.
11. A. INOUE, K. MATSUZAKI, H. S. CHEN and T. MASUMOTO, *J. Mater. Sci.* in press.
12. K. MATSUZAKI, A. INOUE and T. MASUMOTO, unpublished research (1984).
13. T. OTSUKA, "Ferroelectrics and Superconductor", edited by the Japan Institute of Metals (Japan Institute of Metals, Sendai, 1973) p. 131.
14. W. L. JOHNSON, "Rapidly Quenched Metals III", edited by B. Cantor (The Metals Society, London, 1978) p.1.
15. A. INOUE and T. MASUMOTO, *Sci. Rep. Res. Inst. Tohoku Univ.* **A29** (1981) 305.
16. G. DEUTSCHER and D. G. DE GENNES, "Superconductivity", Vol. 2, edited by R. D. Parks (Marcel Dekker, New York, 1969) p. 1005.
17. W. SILVERT and A. SINGH, *Phys. Rev. Lett.* **28** (1972) 222.
18. R. W. ROBERTS, "Properties of Selected Superconductive Materials", 1978 Supplement, NBS Technical Note 983 (US Department of Commerce, Washington).
29. M. LYON and G. ZEPP, *Can. J. Phys.* **55** (1977) 55.
20. W. SILVERT, *Solid State Commun.* **14** (1974) 635.
21. W. SILVERT and L. N. COOPER, *Phys. Rev.* **141** (1966) 336.
22. K. MAKI and T. TSUZUKI, *ibid.* **139** (1965) 868.

Received 30 January
and accepted 13 March 1985